

Enlarged Multilocus Data set Provides Surprisingly Younger Time of Origin for the Plethodontidae, the Largest Family of Salamanders

XING-XING SHEN¹, DAN LIANG¹, MENG-YUN CHEN¹, RONG-LI MAO¹, DAVID B. WAKE^{2,*}, AND PENG ZHANG^{1,*}

¹State Key Laboratory of Biocontrol, College of Ecology and Evolution, School of Life Sciences, Sun Yat-Sen University, Guangzhou, China and ²Museum of Vertebrate Zoology and Department of Integrative Biology, 3101 Valley Life Sciences Bldg, University of California, Berkeley, CA 94720, USA

*Correspondence to be sent to: PZ: #434, School of Life Sciences, Sun Yat-Sen University, Higher Education Mega Center, Guangzhou 510006, China. Tel: + 86 20 39332782; Email: alarzhang@gmail.com; DBW: 3101 Valley Life Sciences Bldg, University of California, Berkeley, California 94720, USA. Tel: 510 643-7705; Email: wakelab@berkeley.edu.

Received 13 August 2014; reviews returned 13 August 2015; accepted 15 August 2015
Associate Editor: Robb Brumfield

Abstract.—Deep phylogenetic relationships of the largest salamander family Plethodontidae have been difficult to resolve, probably reflecting a rapid diversification early in their evolutionary history. Here, data from 50 independent nuclear markers (total 48,582 bp) are used to reconstruct the phylogeny and divergence times for plethodontid salamanders, using both concatenation and coalescence-based species tree analyses. Our results robustly resolve the position of the enigmatic eastern North American four-toed salamander (*Hemidactylium*) as the sister taxon of *Batrachoseps* + Tribe Bolitoglossini, thus settling a long-standing question. Furthermore, we statistically reject sister taxon status of *Karsenia* and *Hydromantes*, the only plethodontids to occur outside the Americas, leading us to new biogeographic hypotheses. Contrary to previous long-standing arguments that plethodontid salamanders are an old lineage originating in the Cretaceous (more than 90 Ma), our analyses lead to the hypothesis that these salamanders are much younger, arising close to the K-T boundary (~66 Ma). These time estimates are highly stable using alternative calibration schemes and dating methods. Our data simulation highlights the potential risk of making strong arguments about phylogenetic timing based on inferences from a handful of nuclear genes, a common practice. Based on the newly obtained timetree and ancestral area reconstruction results, we argue that (i) the classic “Out of Appalachia” hypothesis of plethodontid origins is problematic; (ii) the common ancestor of extant plethodontids may have originated in northwestern North America in the early Paleocene; (iii) origins of Eurasian plethodontids likely result from two separate dispersal events from western North America via Beringia in the late Eocene (~42 Ma) and the early Miocene (~23 Ma), respectively. [Dispersal; molecular dating; paleogeography; phylogenomics; species tree; timetree.]

Lungless salamanders (Plethodontidae) are the most successful radiation in the long evolutionary history of caudate amphibians, comprising more than two-thirds of all living salamander species (AmphibiaWeb 2015). They occupy a surprisingly broad series of ecological niches, from temperate woodlands to deserts and tropical rainforests, and exhibit great diversity in life history, morphology, and ecology. Notably, plethodontids are the only salamanders with an extensive presence in tropical regions. Trait evolution in plethodontids is characterized by pervasive homoplasy (Wake 1966, 1991; Mueller et al. 2004), thus providing an important model system to study macroevolutionary processes, a robust, reliable phylogeny is essential. However, despite recent molecular studies that have built an ever-growing database, a general consensus on the phylogenetic relationships among the major plethodontid lineages is lacking. For example, analyses based on a few nuclear genes (Min et al. 2005; Vieites et al. 2007), whole mtDNA genomes (Mueller et al. 2004) and combined data sets (Chippindale et al. 2004; Kozak et al. 2009; Pyron and Wiens 2011; Vieites et al. 2011) have yielded conflicting results in placing several key genera, especially *Hemidactylium*, *Aneides*, *Ensatina*, *Hydromantes*, and *Karsenia*. This uncertainty about relationships has hindered our understanding of the macroevolutionary processes that underlie plethodontid diversity.

Plethodontids are distributed in a curious and unique, highly disjunct, and asymmetric manner in the Holarctic

region, with 98% of the species in America, a few in the central Mediterranean portion of Europe, and a sole species (*Karsenia koreana*) on the Korean Peninsula (Fig. 1). When and where plethodontids arose, and how and when they achieved their present distribution, remain compelling questions. For example, Appalachia was long thought to be the site of origin of plethodontids, until it was brought into question (Ruben and Boucot 1989; Mueller et al. 2004). Furthermore, the timing and route of colonization of Eurasia by plethodontids has long been a biogeographic enigma (reviewed by Wake 2013). Historically, North America has been connected to Eurasia by the relatively ephemeral Paleocene–Eocene North Atlantic land bridge (NALB) and the long-lasting Bering land bridge (Beringia), so Eurasian plethodontids might have used either route, (NALB: Lanza and Vanni 1981; Delfino et al. 2005. Beringia: Wake et al. 1978; Vieites et al. 2007; Wake 2013. Both: Lanza et al. 2005). However, because the NALB was completely broken after the Late Eocene (~39 Ma), Eurasian plethodontids could not use this route if they originated too late. Reliable estimation of relationships and splitting times are key elements in tackling such questions.

Because early plethodontid fossils are rare, our understanding of the timing of their diversification is based mainly on molecular data. However, recent dating analyses using molecular data have yielded conflicting results. For example, analyses based on whole mtDNA genome sequences (Mueller 2006; Zhang and Wake 2009) suggested that the most recent common ancestor

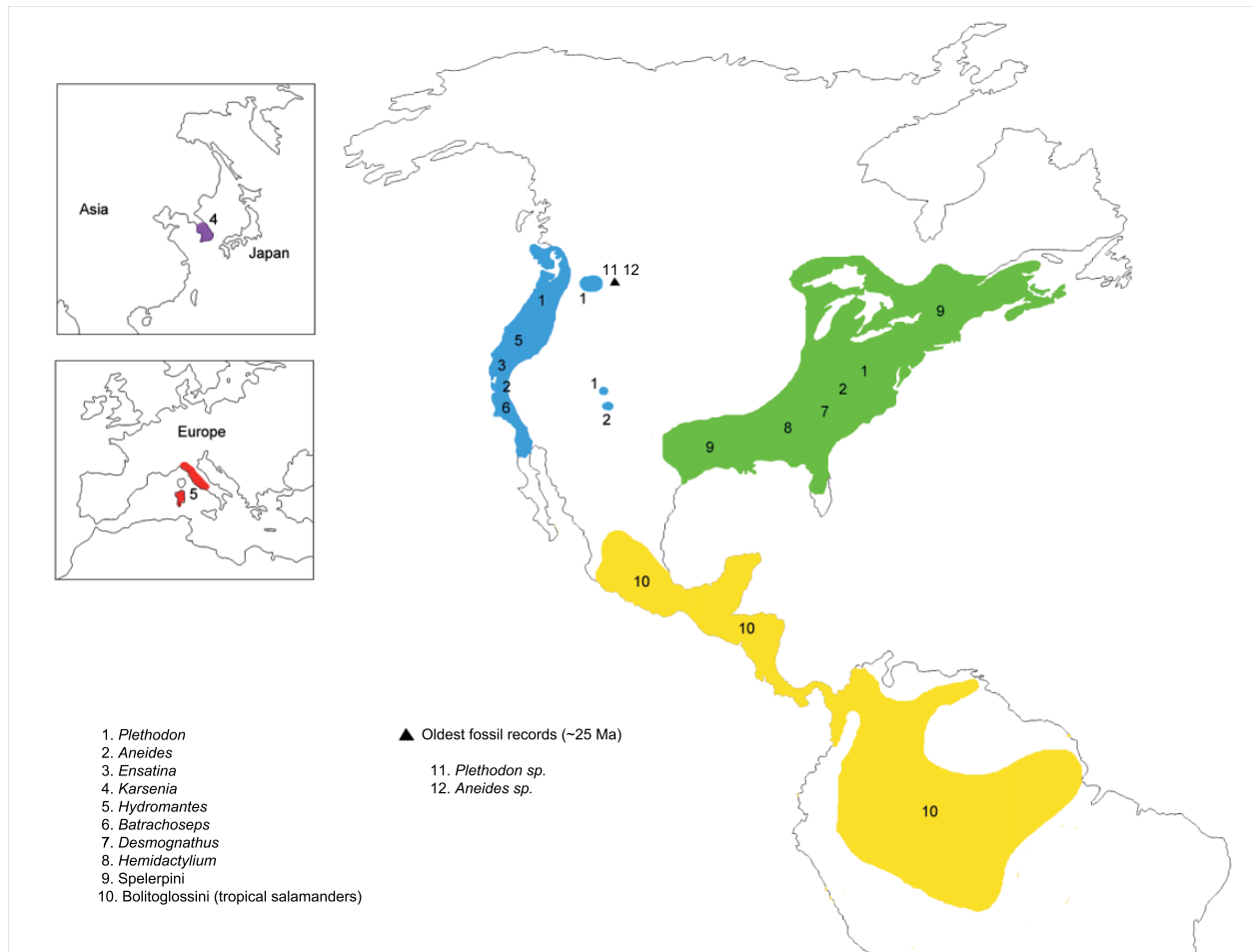


FIGURE 1. Current distribution of extant plethodontid salamanders. The distribution area is roughly divided into five parts: western North America (blue), eastern North America (green), tropical (yellow), East Asia (purple), and central Europe (red). The locality for related fossil taxa is indicated as a black triangle. For color version, please see SYSBIO online.

of living plethodontids occurred 98–129 Ma; however, molecular inferences based on a few nuclear genes (Roelants et al. 2007; Vieites et al. 2007) supported a younger origin of 81–94 Ma. Recent empirical studies have consistently shown that slowly evolving markers such as nuclear exons surpass mitochondrial data for dating a phylogeny covering a relatively wide time span (Zheng et al. 2011; Near et al. 2012). However, because nuclear exons are relatively conservative and contain fewer signal sites, more loci should be used to calculate reliable divergence times (Zheng et al. 2011).

In this study, we generated a large multilocus data set of 50 unlinked nuclear protein-coding genes for 25 plethodontid species and 13 out-group species, covering all major lineages of Plethodontidae. Our goal was to test previously proposed hypotheses on phylogenetic relationships, as well as to estimate divergence times of the main lineages in the family by large-scale data analyses. Our analyses generated new hypotheses of phylogenetic relationships and divergence timing, and provided new perspectives on the evolutionary

history and historical biogeography of plethodontid salamanders.

METHODS

Taxon and Gene Sampling, and Laboratory Protocols

We sampled 25 plethodontid species representing all Holarctic plethodontid genera and all 9 plethodontid tribes (Wake 2012). Currently, Neotropical plethodontids are allocated to 12 genera (AmphibiaWeb 2015) and the monophyly of this group is unquestioned (Mueller et al. 2004; Vieites et al. 2007; Pyron and Wiens 2011; Vieites et al. 2011). Our sampling of Neotropical plethodontids is limited to three genera (*Thori*, *Bolitoglossa*, and *Pseudoeurycea*), which span the entire tree of this group (see Pyron and Wiens 2011). Six additional salamanders, two frogs, and four amniotes are included to provide a backbone phylogeny and calibration points for molecular dating analyses. African lungfish was used as an out-group.

TABLE 1. Summary information for the 50 NPCL amplified in 25 plethodontid salamanders

Gene	Length (bp)	Taxa amplified (%)	GC%	Var. sites	PI sites	Overall mean <i>P</i> distance	Compositional homogeneity (<i>P</i> -value)
ADNP	798	25 (100)	45	218	114	0.0549	1.0000
ANKRD50	903	25 (100)	43	271	136	0.0553	1.0000
CAND1	1119	25 (100)	45	287	178	0.0556	1.0000
CPT2	747	24 (96)	44	301	162	0.0850	1.0000
DBC1	774	25 (100)	51	160	90	0.0424	1.0000
DET1	720	24 (96)	47	187	104	0.0570	1.0000
DISP2	927	25 (100)	44	303	178	0.0696	1.0000
DNAH3	918	24 (96)	42	269	162	0.0628	1.0000
DOLK	738	19 (76)	48	213	102	0.0629	1.0000
DSEL	1266	25 (100)	43	422	237	0.0677	1.0000
ENC1	1071	25 (100)	51	288	188	0.0604	1.0000
EXTL3	1206	25 (100)	46	308	176	0.0541	1.0000
FAT1	1503	25 (100)	41	611	326	0.0804	1.0000
FAT2	936	25 (100)	44	428	252	0.1015	1.0000
FAT4	738	25 (100)	46	260	143	0.0700	1.0000
FEM1B	963	25 (100)	49	321	202	0.0729	1.0000
FLRT3	996	25 (100)	44	269	156	0.0597	1.0000
FREM2	1026	25 (100)	47	366	233	0.0807	1.0000
FUT9	759	25 (100)	41	164	91	0.0445	1.0000
FZD4	783	24 (96)	52	222	149	0.0708	1.0000
HYP	1260	24 (96)	46	368	210	0.0607	1.0000
KCNF1	765	25 (100)	54	219	132	0.0599	1.0000
KIAA1239	1377	24 (96)	42	320	181	0.0516	1.0000
KIAA2013	537	25 (100)	50	172	101	0.0659	1.0000
LIG4	1017	24 (96)	39	301	159	0.0588	1.0000
LINGO1	1071	25 (100)	50	272	148	0.0489	1.0000
LINGO2	1251	24 (96)	46	325	180	0.0498	1.0000
LRRN1	837	24 (96)	48	220	127	0.0595	1.0000
LRRTM4	1110	25 (100)	51	291	174	0.0535	1.0000
MB21D2	993	25 (100)	52	288	181	0.0689	1.0000
MIOS	945	25 (100)	45	249	155	0.0579	1.0000
NHS	849	25 (100)	44	175	86	0.0356	1.0000
PANX2	744	25 (100)	43	171	105	0.0442	1.0000
PCLO	849	24 (96)	42	239	124	0.0563	1.0000
PDP1	1038	25 (100)	44	260	141	0.0515	1.0000
PIK3CG	924	25 (100)	43	363	221	0.0826	0.9973
PPL	1338	25 (100)	44	467	258	0.0661	1.0000
RAG1	1380	25 (100)	49	441	286	0.0733	1.0000
RAG2	900	25 (100)	47	381	212	0.0881	1.0000
ROR2	927	25 (100)	47	256	152	0.0585	1.0000
SACS	1101	25 (100)	40	286	143	0.0495	1.0000
SALL1	1350	25 (100)	46	463	228	0.0638	1.0000
SH3BP4	1140	25 (100)	51	400	244	0.0773	1.0000
SLITRK1	1152	25 (100)	56	376	256	0.0767	1.0000
OCS5	957	25 (100)	47	271	153	0.0566	1.0000
STON2	795	25 (100)	46	221	111	0.0521	1.0000
SVEP1	813	25 (100)	46	319	176	0.0780	1.0000
TTN	984	25 (100)	43	255	155	0.0535	1.0000
ZBED4	1014	25 (100)	38	263	123	0.0484	1.0000
ZHX2	1077	25 (100)	44	390	220	0.0733	1.0000

Note: Length, length of refined alignment; PI sites, parsimony informative sites. *P* distance value is estimated using MEGA5 (Tamura et al. 2011). Compositional homogeneity (*P*-value) is calculated with the X2 test implemented in PAUP* v4.0b10 (Swofford 2002).

Total genomic DNA was extracted from ethanol-preserved tissues (liver or muscle) using a standard salt extraction protocol (Aljanabi and Martinez 1997). All extracted genomic DNA was quantified using the Nanodrop 2000 (Thermo Scientific) and diluted to a concentration of 50 ng/μL. PCR primers used to amplify the 50 nuclear genes were from a recently developed nuclear marker set (Shen et al. 2013). All of the 50 target regions (see Table 1) are nuclear protein-coding

exons. Of the target 1900 sequences, 468 are available in public databases (NCBI and UCSC); 1432 sequences were generated *de novo*. Nuclear genes were amplified with a nested PCR strategy, as described by Shen et al. (2013) and bidirectionally sequenced by Sanger sequencing. All newly obtained sequences were examined by checking for the presence of premature stop codons (pseudogene) and frame-shifting mutations. Detailed information of species, nuclear markers, and GenBank

accession numbers of newly generated sequences are given in Supplementary Table S1 (available on Dryad at <http://dx.doi.org/10.5061/dryad.h4qn5>).

Sequence Alignment, Partition Strategy, and Substitution Model Selection

Each nuclear gene was aligned using the program PRANK v.130410 (Löytynoja and Goldman 2008) according to their translated amino acid sequences (translate). Ambiguous alignment regions were trimmed by using Gblocks 0.91b (Castresana 2000) with type of sequences set to codons ($-t=c$) and half gaps allowed ($-b5=h$); otherwise, default settings were assumed. It should be mentioned here that using GBlocks (or any other alignment-filtering method) may worsen single-gene phylogenetic inference (Tan et al. 2015). However, this argument is still contentious and beyond the scope of our study. Therefore, we still used Gblocks for automated alignment refinement. All 50 refined alignments were combined into a concatenated data set (48,582 bp) and we manually defined five different partitioning schemes: 1 partition (unpartitioned); 3 partitions (a separate partition for all first, second, and third codon positions); 50 partitions (one partition for each gene); 100 partitions (a separate partition for the first and second codon positions together in each gene and a partition for the third codon position in each gene); and 150 partitions (a separate partition for each codon position in each gene). Comparisons of the five partitioning strategies and selections of corresponding nucleotide substitution models were conducted under the Bayesian information criterion (BIC) implemented in PartitionFinder v1.0.1 (Lanfear et al. 2012). The three-partition scheme was chosen as the best-fitting partitioning strategy, and all three partitions favored the GTR+ Γ +I model. The data matrices and resulting trees were deposited in TreeBase (<http://purl.org/phylo/treebase/phyloids/study/TB2:S17263>).

Phylogenetic Analyses

The concatenated data set was separately analyzed with both maximum likelihood (ML) and Bayesian inference (BI) methods using three-codon position partitioning. Partitioned ML analyses were implemented using RAxML version 7.2.8 (Stamatakis 2006), with the GTR+ Γ +I model assigned to each partition. Supports for nodes were assessed with 500 rapid bootstrapping replicates. The partitioned BI was implemented in MrBayes 3.2 (Ronquist et al. 2012). All model parameters were unlinked. Two MCMC (Markov Chain Monte Carlo) runs were performed with one cold chain and three heated chains (temperature set to 0.1) for 60 million generations and sampled every 1000 generations. The chain stationarity was checked by plotting $-\ln L$ against the generation number in Tracer version 1.4 (Rambaut and Drummond 2007). The effective sample

sizes (ESS) are greater than 200 for all parameters after the first 20% of generations were discarded. Topologies and posterior probabilities were estimated from the remaining generations. Two runs for each analysis were compared for congruence.

Species tree analysis without gene concatenation was performed using the pseudo-ML approach implemented in the program MP-EST v1.5 (Liu et al. 2010) under the coalescent model. First, for each nuclear gene, 500 bootstrapping gene trees were constructed using PHYML 3.0 (Guindon et al. 2010) under its best-fitting model, which is selected under the BIC implemented in jModelTest v2.1.7 (Durriba et al. 2012). Second, the gene trees obtained for the 50 nuclear genes were rooted with the lungfish (*Protopterus annectens*) and supplied to the MP-EST to generate 500 bootstrapping species trees. The consensus and robustness of the species tree were evaluated with the 500 bootstrapping replicates.

Likelihood-based tests of alternative phylogenetic hypotheses were assessed based on the concatenated data set. Site-wise log-likelihoods of all alternative hypotheses (see Table 2) were first calculated with RAxML under the GTR+ Γ +I model using the option ($-f g$). Then, the site log-likelihood file was supplied to the CONSEL program (Shimodaira and Hasegawa 2001) to estimate *P*-values for each alternative hypothesis using the approximately unbiased (AU) test, the Kishino-Hasegawa (KH) test, and the bootstrap probability (BP).

Divergence Time Estimation

No consensus prevails concerning which of the many dating procedures using molecular data is the most accurate in time estimation. Accordingly, we used three popular Bayesian relaxed-clock dating programs, MultiDivTime (Thorne and Kishino 2002), MCMCTREE (dos Reis et al. 2014), and BEAST (Drummond and Rambaut 2007) to estimate divergence times. The reference topology was that derived from the ML analysis. All molecular dating analyses were performed with three codon partitions, as in the phylogenetic analyses.

Our analysis began by using three different calibration schemes used by previous studies (Mueller 2006; Vieites et al. 2007; Zheng et al. 2011) in the MultiDivTime analysis (see Supplementary Table S2 for details). Because alternative calibration schemes have little impact on divergence time estimation within living salamanders (Supplementary Fig. S1), we chose the calibration scheme with eleven time constraints used by Vieites et al. (2007) for our definitive molecular dating analyses. Three widely tested nodes were constrained with lower and upper bounds: the Amniota–Amphibia split (332–360 Ma; Benton and Donoghue 2007), the Mammalia–Aves split (312–330 Ma; Benton and Donoghue 2007), and the Aves–Crocodyllia split (243–251 Ma; Benton and Donoghue 2007). Five less defined nodes were constrained with lower bounds only, based on known fossil records: the split between

TABLE 2. Statistical confidence (P -values) for alternative branching hypotheses based on the 50-gene data set

Alternative topology tested	$\Delta \ln L$	P -value			Rejection
		AU	BP	KH	
Best tree	0	0.519	0.075	0.45	— — —
<i>Hemidactylium</i> sister to remaining genera	673.0532	3.00E-04	0	0	+ + +
<i>Hemidactylium</i> sister to (<i>Batrachoseps</i> + <i>Bolitoglossini</i>) + <i>Spelerpini</i>	328.8304	2.00E-07	0	0	+ + +
<i>Hemidactylium</i> sister to <i>Batrachoseps</i>	102.8745	2.00E-42	0	2.00E-04	+ + +
<i>Karsenia</i> sister to remaining subfamily Plethodontinae	7.767544	0.255	0.05	0.348	— — —
<i>Karsenia</i> sister to <i>Plethodon</i>	-1.6251	0.591	0.258	0.478	— — —
<i>Karsenia</i> sister to <i>Hydromantes</i> + <i>Ensatina</i>	47.80727	3.00E-30	0	0.001	+ + +
<i>Karsenia</i> sister to <i>Hydromantes</i>	58.33756	1.00E-142	0	0.002	+ + +
<i>Karsenia</i> sister to <i>Ensatina</i>	65.97841	2.00E-129	0	5.00E-04	+ + +
<i>Karsenia</i> sister to <i>Aneides</i> + <i>Desmognathus</i>	-2.7957	0.658	0.368	0.522	— — —
<i>Karsenia</i> sister to <i>Desmognathus</i>	17.31448	0.045	0.012	0.031	+ + +
<i>Karsenia</i> sister to <i>Aneides</i>	19.88047	0.017	0.003	0.015	+ + +
<i>Ensatina</i> sister to remaining subfamily Plethodontinae	26.29407	0.121	0.026	0.137	- + -
<i>Ensatina</i> sister to <i>Plethodon</i>	38.38214	0.039	0.002	0.051	+ + -
<i>Ensatina</i> sister to <i>Karsenia</i> + <i>Aneides</i> + <i>Desmognathus</i> + <i>Hydromantes</i>	30.25031	0.036	0.002	0.075	+ + -
<i>Ensatina</i> sister to <i>Aneides</i> + <i>Desmognathus</i> + <i>Hydromantes</i>	6.868215	0.355	0.051	0.359	— — —
<i>Ensatina</i> sister to <i>Aneides</i> + <i>Desmognathus</i>	1.170115	0.511	0.152	0.438	— — —
<i>Ensatina</i> sister to <i>Desmognathus</i>	28.15624	0.002	0.001	0.168	+ + -
<i>Ensatina</i> sister to <i>Aneides</i>	26.84005	0.018	0.002	0.181	+ + -
<i>Hydromantes</i> sister to <i>Plethodon</i>	58.38783	0.001	1.00E-05	0.007	+ + +

Note: Best tree refers to Figure 2a; L, likelihood value; AU, approximatedly unbiased test; BP, bootstrap probability; KH, Kishino-Hasegawa test.

Aves and Squamata at least 252 Ma (*Protosaurus speneri*; Evans and King 1993), the split between Anura and Caudata at least 230 Ma (*Triadobatrachus massinoti*; Rage and Rocek 1989), the split between Hynobiidae and Cryptobranchidae at least 155 Ma (*Chunerpeton tianyiensis*; Gao and Shubin 2003), the split between Amphiumidae and Plethodontidae at least 65.5 Ma (*Proamphiuma cretacea*; Gardner 2003), the split between eastern and western *Plethodon* clades at least 25 Ma (Tihen and Wake 1981).

For MultiDivTime analysis, lungfish (*Protopterus annectens*) was used as the out-group and the Amniota-Amphibia split was regarded as the in-group root. For each codon partition, the model parameters were calculated with an F84+ Γ model using the BASEML program in PAML4.8 package (Yang 2007), and optimized branch lengths with their variance-covariance matrices of the DNA data set were estimated by the program Estbranches_dna, a component of MultiDivTime. The priors for the mean (rttm) and standard deviation (rtmsd) of the in-group root age were set to 3.44 and 0.15 time units (1 time unit = 100 Ma), respectively. The prior mean (rtrate) and standard deviation (rtratesd) for the gamma distribution describing the rate at the root node were both set to 0.089. These values were based on the median of the substitution path lengths between the root and each terminal, divided by rttm (as suggested by the authors). The autocorrelation parameter prior (brownmean) and its SD (brownstd) were set to 0.58, such that brownmean multiplied by the rttm prior (3.44) equals 2.0. After an initial burn-in period of 100,000 cycles, MCMC chains were run for 3,000,000 cycles, with sampling intervals of

every 100 cycles. Two independent runs were performed to examine whether similar results were observed.

For MCMCTREE analysis, we used the latest MCMCTREE in the PAML4.8 package which uses a new prior (gamma-Dirichlet prior) to describe substitution rates across multiple loci, thereby improving the accuracy of divergence time estimation (dos Reis et al. 2014). The approximate likelihood method was used for divergence time estimation (see MCMCTREE tutorial). The ML estimates of branch lengths for the three codon partitions were obtained using BASEML (in PAML) programs under the GTR + Γ model. For the gamma-Dirichlet prior for the overall substitution rate (rgene gamma), we used a quite diffuse (uninformative) prior $\alpha_{\mu} = 1$. Based on the mean estimate from three codon partitions using the strict molecular clock assuming 346 Ma constraint at the root, an average of the Amniota-Amphibia split (332–360 Ma; Benton and Donoghue 2007), the gamma-Dirichlet prior for the overall substitution rate (rgene gamma) was set at G (1, 11.96, 1). The gamma-Dirichlet prior for the rate-drift parameter (sigma2 gamma) was set at G (1, 4.5, 1). All eleven calibration constraints were not rigorously constrained (specified with 2.5% tail probabilities above or below their limits; this is a built-in function of MCMCTREE). The independent-rate and autocorrelated-rate models (clock=2 and clock=3 in MCMCTREE) were separately used to estimate divergence time. For each model, after a burn-in period of 2,000,000 cycles, the MCMC run was sampled every 400 cycles until a total of 10,000 samples were collected. Two separate MCMC runs were compared for convergence with two different random seeds and similar results were observed.

For BEAST analysis, we assigned a lognormal relaxed-clock model (uncorrelated), a GTR+ Γ +I site model, and a Yule tree prior for each of the three codon partitions. For calibration points with both minimum and maximum bounds, we used lognormal distributions to describe the priors of those calibration points with maximum boundaries, representing a “soft” calibration strategy. The means and standard deviations of the lognormal distribution for each calibration point were chosen so that 95% of the probability lies within the minimum bound and the maximum bound and the means are the arithmetical medians of the intervals. For the calibration points with only minimum bounds, the means and standard deviations were set so that the lognormal distributions have 2.5% of chance beyond the minimum bound. Two independent runs were performed for 300 million generations, with sampling every 6000 generations. The convergence of the run was confirmed in Tracer version 1.4 (Rambaut and Drummond 2007) because ESS for all parameters are all >200. The two runs reached similar likelihood platforms and results of the two runs were summarized after discarding the first 25% generations.

Historical Biogeography Reconstruction

To test the likelihood of different ancestral distribution scenarios for plethodontid salamanders, ML inference of the evolution of geographic ranges was explored with Lagrange v2.0 (Ree and Smith 2008). We used the plethodontid portion of the time tree generated by our molecular dating analyses as the input time-calibrated phylogeny, which included 25 in-group plethodontid species and two out-groups (Amphiumidae and Rhyacotritonidae). Based on the current distribution pattern of plethodontids (Fig. 1), we defined five possible ancestral distribution areas: western North America (WN), eastern North America (EN), eastern Eurasia (EE), western Eurasia (WE), and tropical region (TP). Although Amphiumidae is currently endemic to southeastern North America, its fossils are found across North America and its oldest fossils are all from WN (reviewed by Bonett et al. 2014). Therefore, we set up two independent analyses that assume Amphiumidae has an ancestral distribution of WN or an ancestral distribution across all of North America, respectively.

Paleogeographic connections between these areas were gathered from the literature. WN is continuously connected to EN except that an epicontinental seaway separated them during the Cretaceous (110–70 Ma) (Blakey 2011). TP was continuously connected to WN and EN but its connection to EN was blocked during the epicontinental seaway period (110–70 Ma) (Blakey 2011). The Beringian land bridge was opening and closing periodically during the Mesozoic and Cenozoic (Tiffney and Manchester 2001), so the connection between WN and EE was also continuous during these periods. The Turgai Sea separated EE from WE from the Middle Jurassic to the Oligocene (160–29 Ma) (Briggs 1995),

beyond that, they connected continuously. The opening of the North Atlantic began in the Late Cretaceous (90 Ma) but terrestrial connections between WE and EN persisted along various North Atlantic land bridges until at least the Late Eocene (39 Ma) (Tiffney 1985). Combining the above information, we set up the probability of dispersal success between two areas to one during the time period they connected, and to zero outside the time period.

For some nodes, except the most probable scenario, Lagrange also gave some alternative biogeographic scenarios with lower likelihood values. In this case, the statistical significance of likelihood differences between biogeographic scenarios was assessed using the conventional cutoff value of two log-likelihood units. Finally, we calculated the relative probability (fraction of the global likelihood) of a certain reported scenario.

Investigating the Effect of Gene Number on Divergence Time Estimation

To investigate the effect of gene number on plethodontid divergence time estimation, we generated data sets with different gene numbers by randomly sampling genes from the whole set of 50 nuclear genes. We generated 200 replicates for each of eight data points with gene number of 3, 6, 12, 24, 50, 100, 150, and 200, respectively (a total number of 1600 data sets). For each data set, divergence times were estimated by MCMCTREE using the independent-rate model (clock=2) and the codon partitioning strategy. All other settings, including calibration choices, follow the MCMCTREE analysis procedure as described before. For the 200 replicates of each data point, the mean divergence times for four representative nodes within the plethodontid timetree (the origin of Plethodontidae, the origin of Hemidactyliinae, the origin of Plethodontinae, and the split between *Hemidactylium* and *Bolitoglossa*) were showed as boxplots.

RESULTS

Data and Phylogenetic Analyses

The supermatrix of 50 combined nuclear genes is 98.5% complete for the 38 taxa and 98.7% complete for the 25 plethodontid taxa (Supplementary Table S1). The aligned lengths of 50 nuclear genes ranged from 540 to 1500 bp (mean = 987). No significant compositional heterogeneity among sequences was detected for any genes among the 25 sampled plethodontid species (Table 1). The combined 50-gene data set comprised 48,582 bp and displays no apparent substitution saturation within the 31 included salamander species (Supplementary Fig. S2).

ML and Bayesian analyses of the concatenated data set and species tree inference without data concatenation produced similar topologies for the

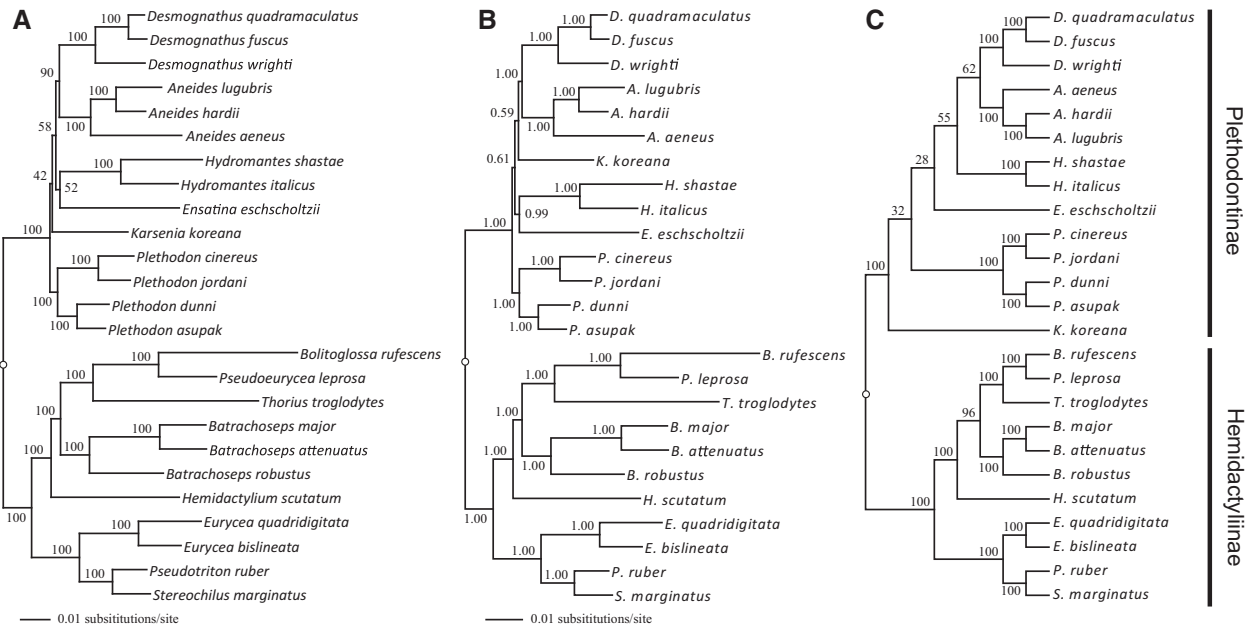


FIGURE 2. Phylogenetic relationships of plethodontid salamanders inferred from 50 nuclear genes (48,582 bp). The trees were inferred by concatenation analyses using ML (a) and BI (b) and by species tree analysis using the MP-EST program (c). Branch support values beside nodes indicate ML bootstrap (a), BI posterior probability (b) and MP-EST bootstrap (c), respectively. The placement of the root of each tree is indicated with an open circle. Out-group taxa are not shown.

25 plethodontid species (Fig. 2). The three analyses all find strong support for the view that plethodontids divided into two major clades (Plethodontinae and Hemidactyliinae), as recovered by most recent molecular studies (Chippindale et al. 2004; Mueller et al. 2004; Frost et al. 2006; Vieites et al. 2007, 2011; Kozak et al. 2009; Pyron and Wiens 2011).

Within the subfamily Hemidactyliinae, the genus-level cladistic structure is well resolved (bootstrap support >95% or PP = 1.0; Fig. 2). The monotypic genus *Hemidactylium* is robustly resolved as the sister taxon of *Batrachoseps* + *Bolitoglossini* (Fig. 2). Within the subfamily Plethodontinae, cladistic structure of the six genera studied is not robustly resolved. However, an *Aneides*+*Desmognathus* clade is strongly supported by ML and Bayesian analyses (Fig. 2a,b). Otherwise, phylogenetic relationships among the remaining four genera are unclear (Fig. 2). The positions of two monotypic genera, *Ensatina* and *Karsenia*, are peculiarly unstable among the three analyses (Fig. 2). Excluding *Ensatina* and *Karsenia*, respectively, from the analyses (Supplementary Figs. S3 and S4) did not provide further resolution for placing these problematic genera. The internal branches separating these genera are extremely short (close to zero), compared to branches elsewhere in the family, suggesting that these ancient cladistic events occurred almost simultaneously.

Divergence Times

In this study, we used four well-known relaxed-clock dating algorithms, MultiDivTime (correlated-rate

model), BEAST (independent-rate model), and MCMCTREE (both independent-rate and correlated-rate models), to calculate divergence times for plethodontids. Because the average time deviation among the four methods is small (~6.4%; see also Table 3), we choose to focus on the results from the MCMCTREE (the independent-rate model; clock = 2) (its time estimates center within the four results) as our preferred dating results. According to the MCMCTREE time estimates, the two major clades of plethodontids began to split at 66.1 (57.8–74.9) Ma (Fig. 3a and Table 3), close to the KT-boundary (~65.5 Ma). This time estimate is 20–50% younger than most previous estimates (at least 80 Ma; e.g., Mueller 2006; Roelants et al. 2007; Vieites et al. 2007; Zheng et al. 2011). The initial diversification of Hemidactyliinae and Plethodontinae took place at 58.6 (51.2–66.6) Ma and 43.1 (37.5–48.7) Ma, respectively. The divergence among major clades of Plethodontinae occurred almost simultaneously within a short time window (~3 myr; Fig. 3a and Table 3).

Ancestral Area Reconstruction

By using the program Lagrange v2.0 (Ree and Smith 2008) and assuming Amphiumidae has an ancestral distribution of WN or an ancestral distribution across North America, we calculated relative probabilities of possible ancestral areas for Plethodontidae, *Karsenia*, all *Hydromantes*, and European *Hydromantes*, respectively.

TABLE 3. Detailed results of Bayesian molecular dating based on the analyses of 50 NPCLs using MultiDivTime, MCMCTREE, and BEAST

Nodes	MCMCTREE			BEAST
	MultiDivTime	Independent-rate model (clock=2)	Correlated-rate model (clock=3)	
1: Amniota–Amphibia ^{344(332–360)}	351.3 (341.0–359.4)	357.5 (350.1–362.5)	354.0 (341.5–362.2)	351.8 (341.8–362.0)
2: Mammalia–Squamata ^{312–330}	319.2 (312.5–327.4)	320.2 (311.9–329.5)	320.4 (311.8–329.5)	320.0 (311.6–328.7)
3: Aves–Squamata ^{>252}	283.7 (277.5–290.9)	278.4 (266.9–290.0)	282.2 (273.2–291.9)	277.9 (267.1–289.7)
4: Aves–Crocodylia ^{243–251}	246.7 (243.2–250.7)	245.6 (242.7–250.2)	246.4 (242.8–250.7)	245.6 (241.2–249.6)
5: Anura–Caudata ^{>230}	320.8 (309.8–331.2)	306.7 (281.6–329.7)	311.4 (284.3–337.5)	296.7 (271.3–323.3)
6: <i>Bombina–Silurana</i>	197.7 (178.6–215.0)	159.2 (128.4–195.3)	154.8 (108.2–206.0)	156.9 (123.2–191.2)
7: Living salamanders	225.3 (206.0–244.7)	196.6 (181.2–212.2)	211.8 (190.9–234.8)	180.2 (157.7–203.5)
8: Hynobiidae–Cryptobranchidae ^{>155}	179.9 (159.1–202.0)	159.6 (155.0–168.1)	167.4 (155.0–186.1)	120.4 (87.7–148.7)
9: Salamandroidea	194.2 (173.8–215.2)	160.5 (144.4–177.4)	177.6 (156.5–200.4)	151.0 (130.7–171.8)
10: <i>Cynops–Ambystoma</i>	174.7 (154.6–195.5)	137.4 (120.2–156.5)	156.1 (135.0–178.5)	128.7 (107.0–148.7)
11: Rhyacotritonidae–Amphiumidae	153.0 (133.0–174.0)	127.9 (113.6–144.6)	144.2 (124.4–166.4)	122.8 (105.7–141.5)
12: Amphiumidae–Plethodontidae ^{>65.5}	129.7 (111.7–148.6)	110.3 (96.1–125.3)	125.5 (105.7–145.8)	106.5 (90.6–122.6)
13: Plethodontinae–Hemidactyliinae	62.7 (50.7–75.6)	66.1 (57.8–74.9)	66.6 (53.0–81.2)	65.1 (56.4–73.0)
14: Plethodontinae	47.0 (37.2–57.9)	43.1 (37.5–48.7)	49.3 (38.6–60.3)	41.3 (35.2–47.2)
15: <i>Karsenia–Aneides</i>	46.1 (36.5–56.8)	42.1 (36.7–47.9)	48.1 (37.5–58.9)	40.5 (34.3–46.2)
16: <i>Aneides–Hydromantes</i>	44.7 (35.4–55.2)	40.7 (35.4–46.3)	46.3 (36.1–56.9)	39.4 (33.5–45.2)
17: <i>Aneides–Desmognathus</i>	43.3 (34.2–53.5)	38.9 (33.4–44.2)	44.7 (34.6–54.8)	37.8 (32.0–43.5)
18: <i>A. aeneus–A. hardii</i>	31.8 (24.8–39.9)	28.2 (23.0–33.6)	32.3 (24.8–40.1)	27.2 (22.2–32.6)
19: <i>A. hardii–A. lugubris</i>	21.3 (16.2–27.5)	18.2 (13.3–23.0)	21.2 (15.9–27.1)	17.4 (12.8–22.0)
20: <i>D. wrighti–D. quadramaculatus</i>	26.8 (20.6–34.0)	20.2 (15.3–25.5)	25.7 (19.0–32.3)	19.7 (14.8–24.8)
21: <i>D. quadramaculatus–D. fuscus</i>	9.7 (6.8–13.4)	6.8 (4.5–9.3)	9.2 (6.4–12.3)	6.6 (4.5–9.1)
22: <i>Ensatina–Hydromantes</i>	43.2 (34.1–53.4)	39.1 (33.6–44.4)	44.5 (34.8–54.8)	37.9 (32.1–43.7)
23: <i>H. italicus–H. shastae</i>	23.4 (17.9–29.8)	23.5 (18.3–28.8)	24.5 (18.4–30.9)	22.6 (17.5–27.7)
24: Eastern–Western <i>Plethodon</i> ^{>25}	43.1 (34.0–53.2)	40.0 (34.2–45.8)	45.3 (35.2–55.4)	37.1 (31.4–43.5)
25: <i>P. dunni–P. asupak</i>	29.5 (22.7–37.5)	20.7 (13.7–28.3)	29.7 (22.2–37.5)	20.6 (14.8–27.6)
26: <i>P. jordani–P. cinereus</i>	20.0 (15.1–25.9)	17.1 (11.7–22.5)	21.3 (15.8–27.5)	16.0 (11.2–21.5)
27: Hemidactyliinae	55.2 (44.2–67.1)	58.6 (51.2–66.6)	58.4 (46.4–71.6)	57.8 (50.2–65.1)
28: <i>Eurycea–Stereochilus</i>	40.0 (31.3–49.6)	37.3 (30.4–44.1)	40.9 (31.6–50.6)	37.0 (29.3–44.0)
29: <i>Stereochilus–Pseudotriton</i>	23.4 (17.5–30.5)	17.7 (12.2–23.2)	22.3 (16.5–28.8)	17.2 (11.9–22.9)
30: <i>E. bislineata–E. quadridigitata</i>	18.4 (13.7–24.1)	18.7 (13.6–24.1)	19.7 (14.1–25.3)	18.3 (13.3–24.0)
31: <i>Hemidactylium–(Batrachoseps+ Bolitoglossini)</i>	50.2 (40.0–61.3)	54.3 (47.0–61.9)	52.9 (41.4–64.7)	53.3 (46.2–60.5)
32: <i>Batrachoseps–Bolitoglossini</i>	47.6 (37.8–58.2)	51.2 (44.0–58.5)	50.0 (39.1–61.4)	50.3 (43.2–57.3)
33: <i>Thorius–Bolitoglossa</i>	38.7 (30.6–47.8)	40.9 (34.1–47.8)	40.0 (31.1–49.4)	40.2 (33.5–46.9)
34: <i>Bolitoglossa–Pseudoeurycea</i>	21.9 (16.8–27.9)	24.9 (19.0–31.1)	23.8 (18.2–30.3)	23.1 (18.4–29.8)
35: <i>B. robustus–B. attenuatus</i>	37.6 (29.6–46.4)	39.6 (33.2–47.2)	39.9 (31.1–49.4)	39.2 (32.3–46.2)
36: <i>B. attenuatus–B. major</i>	14.1 (10.6–18.2)	17.1 (12.3–22.1)	15.2 (11.0–19.9)	16.8 (12.0–22.1)

Node numbers refer to Figure 3a. Eight nodes are labeled with their corresponding age constraints. Values are mean estimates and 95% credible interval (within parentheses). Time unit: 1 myr

When assuming Amphiumidae has an ancestral distribution across North America, EN is the most probable ancestral area for Plethodontidae (rel. prob. = 0.458; Fig. 3b), but WN is the second probable ancestral area for Plethodontidae (rel. prob. = 0.250; Fig. 3b). However, if assuming Amphiumidae has an ancestral distribution of WN, WN is the most probable ancestral area for Plethodontidae (rel. prob. = 0.557; Fig. 3b). Under this assumption, EN becomes the least probable ancestral area for Plethodontidae (rel. prob. = 0.110; Fig. 3b), considerably less likely than the WN hypothesis.

For the Korean *Karsenia*, the most probable ancestral area is WN (rel. prob. ~0.8; Fig. 3b) rather than EE (rel. prob. <0.2; Fig. 3b). *Hydromantes* may have originated in WN (rel. prob. >0.9; Fig. 3b) and the ancestor of European *Hydromantes* most likely lived in EE (rel. prob. >0.9; Fig. 3b).

DISCUSSION

Phylogeny of Plethodontids

The placement of the enigmatic four-toed salamanders of the monotypic genus *Hemidactylium* is one of the most compelling questions in plethodontid phylogenetics. It has been suggested to be the sister taxon to all other plethodontids (Macey 2005), to *Batrachoseps* (Mueller et al. 2004), to all other hemidactyliine plethodontid salamanders (Wake 1966; Chippindale et al. 2004; Kozak et al. 2009; Pyron and Wiens 2011), and to *Batrachoseps* + *Bolitoglossini* (Vieites et al. 2007). By assembling all available molecular data at that time (complete mitochondrial genomes and three nuclear genes), Vieites et al. (2011) placed *Hemidactylium* as the closest relatives of *Batrachoseps*, with an alternative but less likely placement as the sister taxon of *Batrachoseps* + *Bolitoglossini*. These contradictory results may be due to

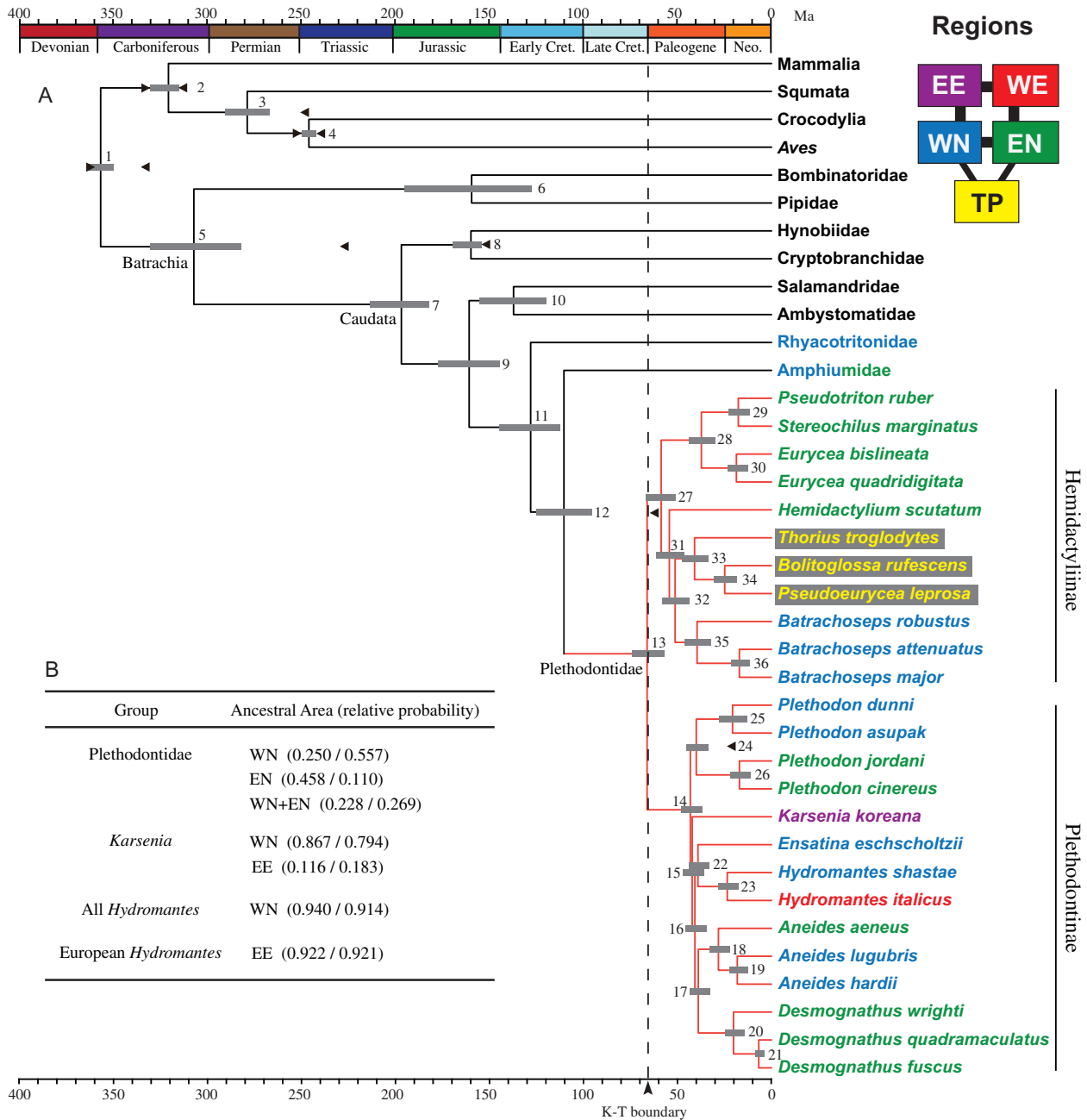


FIGURE 3. Timetree and ancestral area reconstruction results. a) Evolutionary timetree inferred by MCMCTREE using an independent rate model (clock=2). Eleven time constraints used in the molecular dating are shown as black triangles. Gray horizontal bars represent 95% credibility intervals. At the top right, a color-coded square represents the five main regions considered: EE (purple), eastern Eurasia; WE (red), western Eurasia; WN (blue), western North America; EN (green), eastern North America; TP (yellow), tropical region. The same color-coding scheme was applied to species names. Detailed divergence time estimates for nodes with numbers are provided in Table 3. b) Inferences about the ancestral distribution area of four plethodontid groups calculated by Lagrange v2.0. Two probability values are given for every possible ancestral area, assuming that Amphiumidae has an ancestral distribution of whole North America (left) or an ancestral distribution of western North America (right), respectively. For color version, please see SYSBIO online.

rapid evolution and high heterogeneity of mitochondrial genomes and the fact that mitochondrial genomes have a strong numerical advantage in characters over a few nuclear genes. Our concatenation and species tree analyses based on 50 nuclear genes strongly support *Hemidactylum* as the sister taxon to *Batrachoseps*

+ *Bolitoglossini* (MLBS = 100%, BPP = 1.00; Fig. 2). This result remained stable when mitochondrial genome data were added to the analyses (Supplementary Fig. S5). Importantly, all other possible hypotheses about the placement of *Hemidactylum* can be rejected by an AU test (Table 2).

Earlier molecular studies recovered the Asian genus *Karsenia* as the sister group of *Hydromantes*, although without strong support (Vieites et al. 2007; Kozak et al. 2009; Vieites et al. 2011). Contrary to this result, none of our analyses supported such a relationship. Moreover, the AU test statically rejects the grouping of *Karsenia* and *Hydromantes* ($P=0.001$; Table 2), showing that these taxa have no direct genetic affinity. Although not fully resolved, the degree of resolution in our phylogeny among the rapidly diverging Plethodontinae is nevertheless encouraging, and holds promise that using increasingly large numbers of nuclear genes may lead to better phylogenetic resolution of these challenging deep nodes.

Younger Time Estimation for Plethodontid Origin and Diversification

Prior to this study, many attempts had been made to estimate times for the origin and diversification of plethodontids (Mueller 2006; Roelants et al. 2007; Vieites et al. 2007; Wiens 2007; Pyron 2010, 2011; Zheng et al. 2011). Analysis of complete mitochondrial genomes (Mueller 2006) provided estimates for the origin of plethodontids at about 129 (109–152) Ma. As part of a large-scale divergence time study of all amphibians, Roelants et al. (2007) estimated the origin time for plethodontids at 82 (62–103) Ma, based on four nuclear genes and one mtDNA fragment. Using data from three nuclear genes, Vieites et al. (2007) obtained an estimate of 94 (74–117) Ma. By using the three nuclear genes from Vieites et al. (2007) but calibration choices similar to those of Mueller (2006), Zheng et al. (2011) obtained a slightly younger time of 87 (72–100) Ma. Despite differences in time estimates, all four previous studies suggest that plethodontids originated at least 80 Ma, in the Cretaceous. In addition, there are also some younger estimates for plethodontid origin: ~60 Ma (Wiens 2007), and ~70 Ma (Pyron 2010). Moreover, by using fossils as terminal taxa, Pyron (2011) proposed a much younger origin (~40 Ma) for plethodontids. However, these younger estimates are based only on a single nuclear locus (RAG1).

We estimate considerably younger times of divergence than the majority opinion (20–50% younger); the new estimates are to some degree close to previous young estimates. Furthermore, our time estimates (Fig. 3a and Table 3) coincide with all currently known plethodontid fossil records. For example, the oldest stratum that contains uncontroversial plethodontid fossils is the Cabbage Patch formation dated to ~25 Ma (Tihen and Wake 1981; Caledo J., personal communication). Both western *Aneides* and western *Plethodon* were found in this layer, which means the western and eastern groups of both *Aneides* and *Plethodon* separated from each other before or near that date (that is, ca. 25 Ma). Our estimates of divergence between eastern and western *Plethodon* are 40 Ma (node 24, Fig. 3a and Table 3), and 28.2 Ma (node 18, Fig. 3a and Table 3) between eastern and western

Aneides, which fits the fossil data. In addition, the oldest European *Hydromantes* fossil is known from the Middle Miocene of Slovakia (~14 Ma; Venczel and Sanchíz 2005), but previous time estimates suggested that European *Hydromantes* was at least 40 Ma (Mueller 2006; Vieites et al. 2007). Our results find that European *Hydromantes* arose no earlier than 24 Ma (node 23, Fig. 3a and Table 3), which is more congruent with the fossil record.

But could our young time estimates for plethodontids be a methodological artifact? Molecular time estimates can be affected by three major factors: data, calibration scheme, and dating method. Because the average time deviation among the four relaxed-clock methods used in this study is small (~6.4%), the choice of dating methods should have little effect on our time estimates. With respect to calibration schemes, our analyses show that, when using the same dating program and calibration scheme, our molecular time estimates using the 50-gene data sets largely agree with previous studies for the four older salamander nodes outside plethodontids, but are clearly younger for the four nodes within plethodontids (Fig. 4). This discrepancy remains when we successively applied three different calibration schemes used by previous studies to our dating analyses (Fig. 4). Such a phenomenon is likely because the nodes outside plethodontids are relatively tightly constrained by the working calibration points; however the nodes within plethodontids do not have such constraints. Meanwhile, further analyses suggest that using different calibration schemes has no obvious effect on both mean and 95% CI for all 24 nodes within plethodontids (Supplementary Fig. S1). These findings strongly suggest that our time estimates for plethodontids are robust against dating methods and calibration choices, and the younger result is mainly caused by the time signals within our data.

The Effect of Gene Number on Plethodontid Divergence Time Estimation

We have demonstrated that our young time estimates for plethodontids are mainly caused by the data, in other words, the number of genes used. Considering that we only used a modest number of nuclear genes (50 loci here), one may wonder what we will obtain if we use different numbers of genes. Can we get the same time results when we analyze 100 or even more nuclear genes? To answer these questions, we generated simulated data sets with different gene numbers by randomly sampling genes from the whole set of 50 nuclear genes and repeated our time estimation process (see section 'Methods' for details).

Our data simulation shows that when the number of genes goes up from 200 to 300, the median time estimates (from 200 replicates) for the four major plethodontid evolutionary events are all close to what we obtained by using 50 loci (Fig. 5). This result suggests that our dating results are robust against the number of genes used; similar time estimates for plethodontids might well be obtained using 100 or even more nuclear genes.

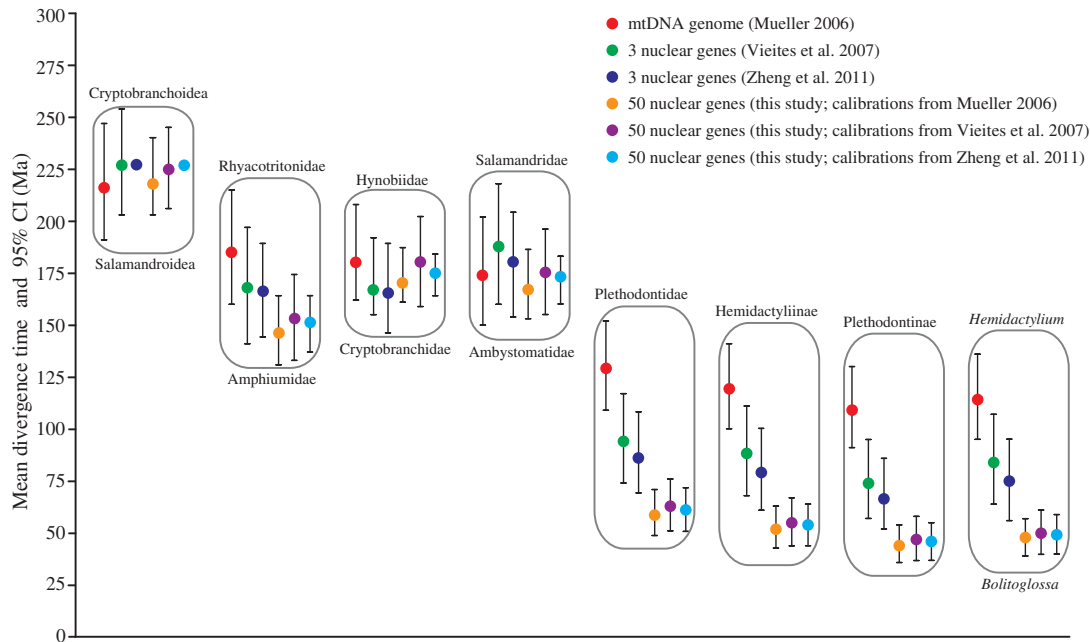


FIGURE 4. Comparison of divergence time estimates for eight split events sharing across four studies. Each box represents a splitting event with its two branching lineages (if applicable) shown above and below the box. The circle within boxes represents the mean of the posterior estimate and the whiskers mark the upper and lower 95% highest posterior density of the age estimates. The comparison shows that (1) our age estimates remain stable when calibration schemes changed; (2) our new age estimates are largely congruent with previous studies for nodes outside plethodontids, but younger within plethodontids.

However, the distribution of time estimates becomes considerably wider when fewer and fewer genes are used (Fig. 5). Notably, using only three nuclear genes, the time estimate for plethodontid origin can be from 48 to 106 Ma (Fig. 5). This observation coincides with previous empirical studies that used a few nuclear genes: 82 Ma, four nuclear genes (Roelants et al. 2007); 94 Ma, three nuclear genes (Vieites et al. 2007); 87 Ma, three nuclear genes (Zheng et al. 2011). Overall, according to our simulation, it is possible to obtain accurate time estimates by using a few genes; however, this practice is prone to random errors because of limited gene sampling.

Our results support the recent argument that analyzing many nuclear loci improves the precision of posterior time estimation (Mulcahy et al. 2012; Zhu et al. 2015). These results not only have important implications for future molecular dating practices for non-model animals, but also raise questions for many molecular dating studies in the past. Previous studies have repeatedly shown that, in the absence of younger effective calibration points, mitochondrial genes tend to overestimate divergence times compared with results from more slowly evolving nuclear genes (Zheng et al. 2011; Near et al. 2012). Therefore, nuclear genes are normally the preferred data source in molecular dating, especially for relatively ancient evolutionary events. However, as indicated by our data simulation, using only a small number of nuclear genes (one to three, as in many recent studies) for molecular dating is risky because of random errors and is likely to produce inaccurate time estimates, especially when the in-group has a relatively

ancient root age but lacks younger calibration points (like the case of plethodontids). This phenomenon was also observed in the molecular dating practices for mammal evolution: the time estimate for *Mus-Rattus* divergence decreases from 23 Ma (3 nuclear genes; Adkins et al. 2001) to 16 Ma (19 nuclear genes; Springer et al. 2003), and eventually to 14 Ma (>14,000 nuclear genes; dos Reis et al. 2012). Because of the historical difficulty in generating large nuclear gene data sets for non-model animals, many molecular dating analyses are still based on a handful of mitochondrial genes and one to three nuclear genes. These dating practices become highly questionable and many of the time estimates may be far too old. We suggest that any applications of those time estimates (e.g., biogeographic hypotheses) should be interpreted with caution until new analyses using more nuclear loci have confirmed them.

Origin of Plethodontids and Historical Biogeography

Plethodontids long were thought to have originated from Appalachia (EN) because loss of lungs was thought to have evolved in mountain streams and this mountain system is old and stable. Furthermore, larvae were thought to be an ancestral state for the family and taxa with fully representation there. Appalachian plethodontids exhibit high present-day cladistic diversity, adaptive diversity, and species richness (Wilder and Dunn 1920; Wake 1966; Beachy and Bruce 1992), further evidence to many is that

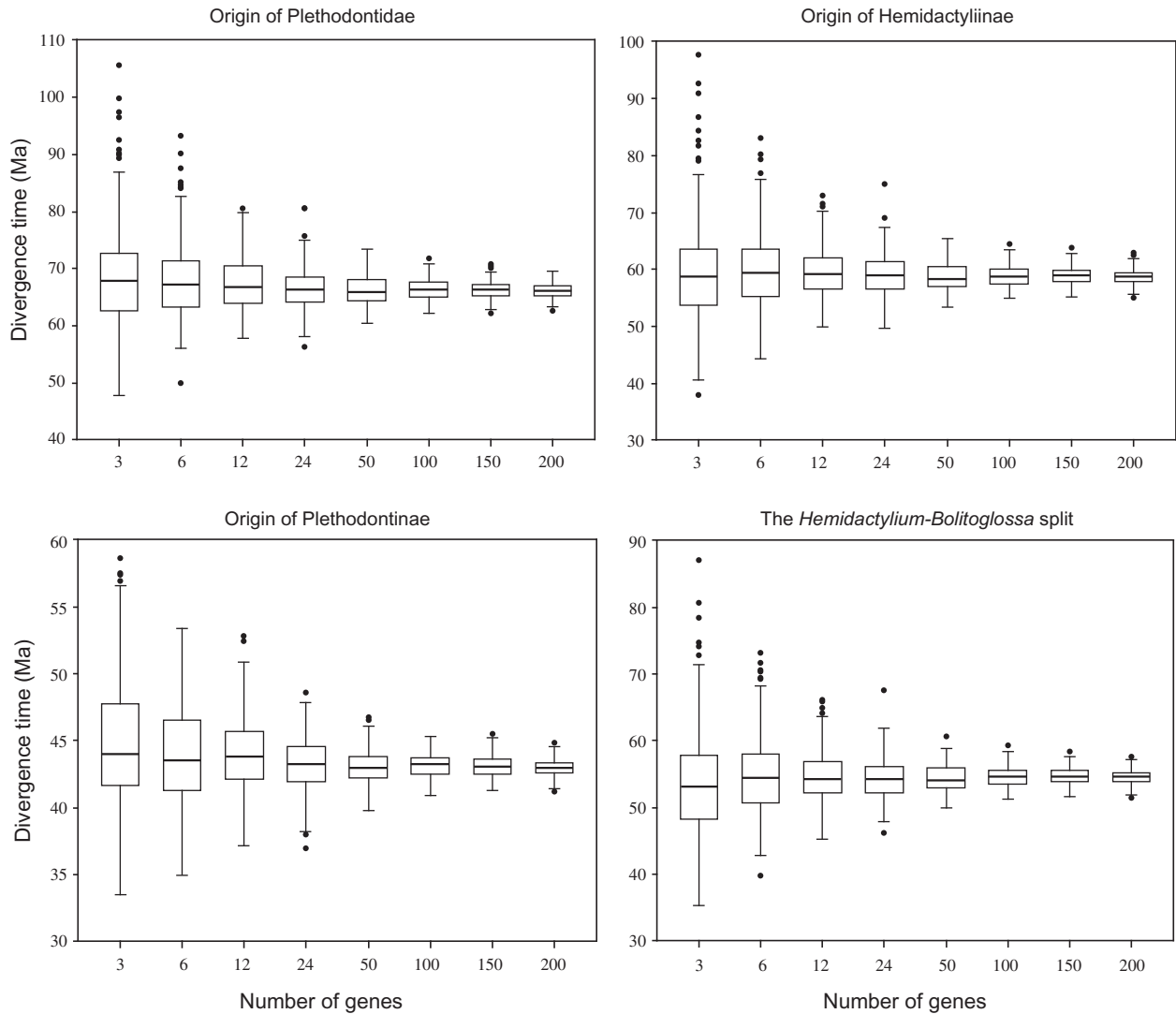


FIGURE 5. Box plot depicting the simulated time estimates for four major evolutionary events of plethodontids. Each box plot contains the time estimates resulted from 200 simulated data sets with different numbers of genes. Box plots show a thick line at the median time estimate, a surrounding box containing the middle 50% of the data, and whiskers extending to encompass the middle 95% of the data. Dots indicate outlier points.

this area is not only the region of origin but also the area in which primary diversification occurred. This idea was further supported by analyses in the context of both geologic history (Beachy and Bruce 1992) and molecular phylogeny (Macey 2005), and thus is widely accepted. However, the “Out of Appalachia” hypothesis was challenged with the discovery of the basal split between two major clades: eastern American Hemidactyliinae and western American Plethodontinae. Mueller et al. (2004) proposed a transcontinental North American origin of plethodontids and Vieites et al. (2007) further inferred that the basal split of plethodontids was caused by a major vicariant event associated with the forming of a midcontinental seaway in North America from 110 to 70 Ma. These biogeographic inferences are largely based on estimates of a Cretaceous divergence between the eastern Hemidactyliinae and the western

Plethodontinae (Mueller 2006; Vieites et al. 2007). Based on our revised time estimate for the basal plethodontid split (~66 Ma), the mid-continental seaway may not have been the driving factor because the seaway, while still partially in existence, was closing rapidly at about 65 Ma (Blakey 2011).

The current distribution of plethodontids does not retain any clues on their early biogeographic history because the major clades, Plethodontinae and Hemidactyliinae, both having representatives in EN and WN (Fig. 1). Although high species and ecological diversity is observed in the Appalachian Mountains, this pattern can be misleading for inferring center of plethodontid origin if the distributions of the relevant fossils are not considered. In fact, Appalachian fossil plethodontids are no older before Mio-Pliocene (~7 Ma; Boardman and Schubert 2011), whereas the

oldest fossil plethodontids (*Aneides* sp. and *Plethodon* sp.) were found in WN (Montana) in late Oligocene (~25 Ma; [Tihen and Wake 1981](#)). For Amphiumidae (the closest extant relative of plethodontids), although it is currently endemic to southeastern North America, the oldest fossil record of this family was also found in WN (*Proamphiuma cretacea*; Cretaceous of Montana, ~65 Ma). Notably, other American salamander families all have similar patterns: Sirenidae (oldest fossil *Habrosaurus prodilatus* from Cretaceous of Alberta, Canada), Dicamptodontidae (oldest fossil *Dicamptodon antiquus* from Paleocene of Alberta, Canada), and Ambystomatidae (oldest fossil *Ambystoma tihenii* from Eocene of Saskatchewan, Canada). These fossil records suggest that the most likely ancestral area for these American salamander families (including Amphiumidae) is WN. The apparent western bias on early fossil distributions of both plethodontids and relevant salamander families suggests that WN could also be the ancestral area for the origin of plethodontids. In fact, when assuming that Amphiumidae has an ancestral distribution of WN, our Lagrange analyses (Fig. 3b) did suggest that WN is the most probable ancestral area for Plethodontidae (rel. prob. = 0.557; Fig. 3b), and both an EN (rel. prob. = 0.110; Fig. 3b) and an origin across the whole North American (WN+EN) (rel. prob. = 0.269; Fig. 3b) have lower probabilities.

Multiple studies have suggested that salamanders originated in Asia with later expansion into America ([Gao and Shubin 2001](#); [Zhang et al. 2005](#)). Given that a very well-supported clade Rhyacotritonidae+(Amphiumidae, Plethodontidae) was consistently recovered by all recent studies ([Roelants et al. 2007](#); [Zhang and Wake 2009](#); [Shen et al. 2013](#)), the common ancestor of Rhyacotritonidae, Plethodontidae, and Amphiumidae most probably dispersed into WN through Beringia (Fig. 6a). The exclusive WN distribution for Rhyacotritonidae adds more force to this hypothesis. The splits among the three salamander families are dated in the mid-Cretaceous (Table 3), a time when EN and WN were separated by an intracontinental seaway (Fig. 6a). Therefore, Rhyacotritonidae, Plethodontidae, and Amphiumidae were likely restricted to WN until the seaway finally closed at the end of the Cretaceous. [Bonett et al. \(2013\)](#) proposed that amphiumids arose in WN in association with the evolution of the Western Interior Coastal Plain, as the intracontinental seaway closed. It is likely that rhyacotritonids and plethodontids also arose in montane areas bordering this plain.

From the late Cretaceous to Paleocene, the climate of North America was ~10 °C warmer than today with palm trees growing in Greenland ([Scotese 2001](#)). The climate in southern North America was generally subtropical to tropical, with high temperatures and rainfall, and with small seasonal differences between summer and winter. This warm phase had begun in the Cretaceous period, peaked in the early Eocene, and continued to the end of the Eocene ([Zachos et al. 2001](#)). Because salamanders are generally cool-adapted, the

common ancestor of plethodontids most likely occurred well to the north, in northwestern North America (Fig. 6a).

Our general hypothesis for the dispersion of plethodontids postulates several steps. After the mid-continental seaway through North America finally closed at the end of the Cretaceous ([Blakey 2011](#)), plethodontids began to spread across the continent and adapted to any available ecological niches. This phase lasted from the Paleocene to the end of the Eocene (65–33 Ma) and produced most major plethodontid lineages. Because southern North America was too hot for salamanders during this period, the major divergences of plethodontids most likely took place in the northern regions of North America (Fig. 6b). As the climate continued to cool in the Oligocene, plethodontids migrated to the south (Fig. 6c). Finally, the increasing aridity of central North America during the Miocene interrupted the former continuous distribution of plethodontids, which split into two major clades, the plethodontines along the western coast area and the hemidactyliines in EN, centered in Appalachia (Fig. 6d). Previous studies argued that the high species diversity of *Plethodon* and *Desmognathus* in Appalachia corresponds mainly to recent radiations ([Kozak et al. 2005](#); [Wiens et al. 2006](#)). We agree with this argument and further suggest that the rapid species accumulation for these genera occurred within the Miocene. Currently, the earliest fossils of plethodontids from Appalachia, including *Plethodon* and *Desmognathus*, date back only to Mio-Pliocene ([Boardman and Schubert 2011](#)).

Origin of Eurasian Plethodontids and Dispersal Routes

The current distribution of plethodontids is disjunctive and highly asymmetric, with 98% of the species in Americas, a few in Europe, and a sole species *Karsenia koreana* in East Asia. More surprisingly, members of the genus *Hydromantes* are distributed in WN and in Europe and the American species and European species of the genus are genetically more closely related to each other than to other plethodontid taxa. How plethodontids attained their present distributions has long been a biogeographic enigma, given their generally low dispersal capability.

Recent molecular studies suggested, although without strong support, that *Karsenia* and *Hydromantes* are sister taxa and they together constitute the initial branch of Plethodontinae ([Vieites et al. 2007, 2011](#)). If these relationships are real, *Karsenia* and *Hydromantes* may have entered Eurasia separately from North America, or by a more likely biogeographic scenario as proposed by [Vieites et al. \(2007\)](#): their common ancestor entered Asia and underwent diversification there, which separated the two genera and left *Karsenia* in northeast Asia. Later, *Hydromantes* migrated both into western Europe and back into WN, and eventually went extinct in Asia. Our phylogenetic analyses based on much more data find no support for the hypothesis that *Karsenia* and

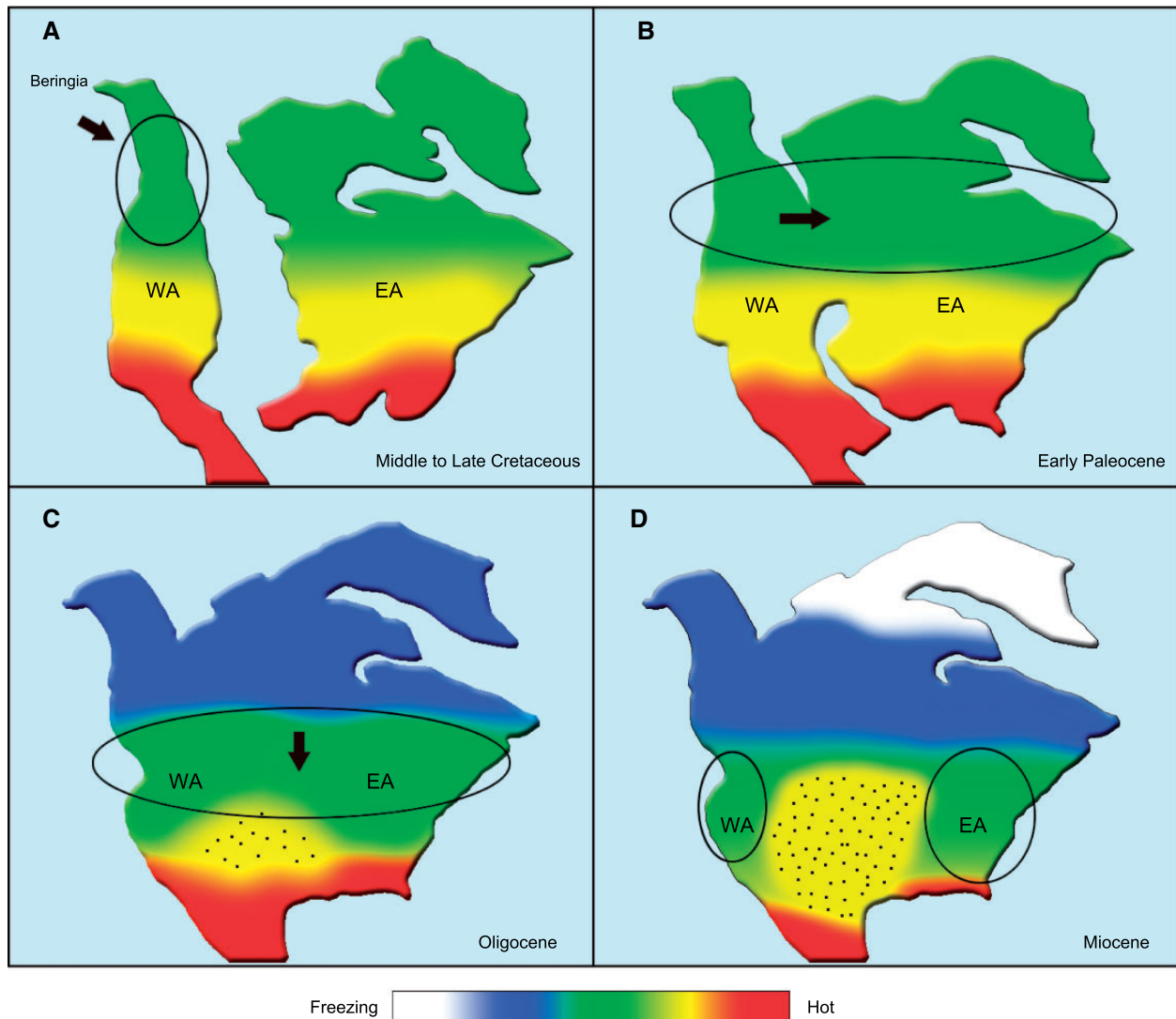


FIGURE 6. Biogeographic hypothesis showing the origin and dispersal pattern of plethodontid salamanders. Landmasses are abbreviated as follows: western North America (WA), eastern North America (EA). a) Ancestors of Amphiumidae and Plethodontidae dispersed into North America by way of Beringia and were restricted to the northern part of WA. b) Plethodontids began their initial diversification and dispersed eastward after the Central Continental Seaway quickly closed in Paleocene. c) Plethodontids migrated southward when the northern North America continued to cool down during Oligocene. d) Plethodontids were restricted to EN and WN as central North America became increasingly dryer in the Miocene (yellow stippled areas mean dry regions).

Hydromantes are sister taxa; rather they are embedded in a near polytomy within the subfamily Plethodontinae, which possesses an otherwise entirely North American distribution. In addition, our ancestral distribution reconstruction also suggests that a WN origin (rel. prob. ~ 0.8 ; Fig. 3b) is much more possible than an East Asian origin (rel. prob. ~ 0.2 ; Fig. 3b) for *Karsenia*. These results make the latter biogeographic scenario proposed by Vieites et al. (2007) highly unlikely, but suggest that the origin of *Karsenia* may have resulted from a dispersal event out of North America.

Although it is generally assumed that the genus *Hydromantes* dispersed into Europe from North America, there is no consensus on the timing and dispersal route for the event (Wake et al. 1978; Lanza et al. 1995; Delfino

et al. 2005; Vieites et al. 2007; Carranza et al. 2008; Wake 2013; Pyron 2014). Geographically, Europe was connected with North America via the North Atlantic Land Bridge (NALB) but separated from Asia by the Turgai Strait from Paleocene to Eocene; with the breakup of NALB and the closure of the Turgai Strait during the Oligocene, the physical connection between Europe and North America was exclusively by way of the Bering Land Bridge (Beringia) via the Asian continent (Jones 2011). Therefore, the time for separation between the American and European *Hydromantes* becomes the key: times no later than Eocene offer some support for the NALB as the dispersal route while times after Oligocene will favor Beringia. A single vertebra of *Hydromantes* (diagnosable as *H. (Speleomantes)* sp.) is

known from the Miocene of Slovakia, dated 13.75 Ma (± 1.25 Ma) (Venczel and Sanchíz 2005), suggesting that the separation between the American and European *Hydromantes* predated this time. Our time estimate for this split is about 23 Ma, congruent with the fossil record. This result also suggests that *Hydromantes* arrived in Europe from North America by crossing Beringia and the entire Asian continent in Miocene. Our biogeographic inferences support this idea because the ancestral distribution area of all *Hydromantes* is exclusively WN (rel. prob. >0.9 ; Fig. 3b), while the ancestral distribution area of European *Hydromantes* is exclusively EE (rel. prob. >0.9 ; Fig. 3b).

SUPPLEMENTARY MATERIALS

Data available from the Dryad Digital Repository: <http://dx.doi.org/10.5061/dryad.h4qn5>.

FUNDING

This work was supported by National Natural Science Foundation of China (grants No. 31372172 and No. 31172075 to P. Zhang) and the National Science Fund for Excellent Young Scholars of China to P. Zhang (No. 31322049).

ACKNOWLEDGMENTS

We thank Chris Evelyn, Elizabeth Jockusch, Ron Bonett, and the P. Zhang laboratory group for discussion and comments. Two anonymous reviewers gave insightful comments that significantly improved this paper. We also thank the editors for their valuable feedback. Finally, tissue samples were provided by the Museum of Vertebrate Zoology, we want to thank those researchers who collected and kindly shared these invaluable specimens.

REFERENCES

- Adkins R.M., Gelke E.L., Rowe D., Honeycutt R.L. 2001. Molecular phylogeny and divergence times for major rodent groups: evidence from multiple genes. *Mol. Biol. Evol.* 18:777–791.
- Aljanabi S.M., Martinez I. 1997. Universal and rapid salt-extraction of high quality genomic DNA for PCR-based techniques. *Nucleic Acids Res.* 25: 4692–4693.
- AmphibiaWeb. 2015. Information on Amphibian Biology and Conservation. Available from: URL <http://amphibiaweb.org/> (accessed 7 August 2015).
- Beachy C.K., Bruce R.C. 1992. Lunglessness in plethodontid salamanders is consistent with the hypothesis of a mountain stream origin: a response to Ruben and Boucot. *Amer. Nat.* 139:839–847.
- Benton M.J., Donoghue P.C. 2007. Paleontological evidence to date the tree of life. *Mol. Biol. Evol.* 24:26–53.
- Blakey R.C. 2011. Paleogeography and Geologic Evolution of North America. Available from: URL <http://jan.ucc.nau.edu/rcb7/nam.html>.
- Boardman G.S., Schubert B.W. 2011. First Mio-Pliocene salamander fauna from the southern Appalachians. *Palaeontol. Electron.* 14:16A.
- Bonett R.M., Steffen M.A., Robison G.A. 2014. Heterochrony repolarized: a phylogenetic analysis of developmental timing in plethodontid salamanders. *EvoDevo* 5:27.
- Bonett R.M., Trujano-Alvarez A.L., Williams M.J., Timpe E.K. 2013. Biogeography and body size shuffling of aquatic salamander communities on a shifting refuge. *Proc. R. Soc. B* 280:20130200.
- Briggs J.C. 1995. *Global Biogeography*. Amsterdam: Elsevier Science.
- Carranza S., Romano A., Arnold E.N., Sotgiu G. 2008. Biogeography and evolution of European cave salamanders, *Hydromantes* (Urodela: Plethodontidae), inferred from mtDNA sequences. *J. Biogeogr.* 35:724–738.
- Castresana J. 2000. Selection of conserved blocks from multiple alignments for their use in phylogenetic analysis. *Mol. Biol. Evol.* 17:540–552.
- Chippindale P.T., Bonett R.M., Baldwin A.S., Wiens J.J. 2004. Phylogenetic evidence for a major reversal of life-history evolution in plethodontid salamanders. *Evolution* 58:2809–2822.
- Darriba D., Taboada G.L., Doallo R., Posada D. 2012. jModelTest 2: more models, new heuristics and parallel computing. *Nat. Methods* 9:772.
- Delfino M., Razzetti E., Salvidio S. 2005. European plethodontids: paleontological data and biogeographical considerations. *Ann. Mus. Civ. Stor. Nat. Genova* XCVII:45–58.
- dos Reis M., Inoue J., Hasegawa M., Asher R.J., Donoghue P.C., Yang Z. 2012. Phylogenomic datasets provide both precision and accuracy in estimating the timescale of placental mammal phylogeny. *Proc. R. Soc. B* 279:3491–3500.
- dos Reis M., Zhu T., Yang Z. 2014. The impact of the rate prior on Bayesian estimation of divergence times with multiple loci. *Syst. Biol.* 63:555–565.
- Drummond A.J., Rambaut A. 2007. BEAST: Bayesian evolutionary analysis by sampling trees. *BMC Evol. Biol.* 7:214.
- Evans S.E., King M.E. 1993. A new specimens of *Protorosaurus* (Reptilia: Diapsida) from the Marl Slate (Late Permian) of Britain. *Proc. Yorkshire Geol. Soc.* 49:229–234.
- Frost D.R., Grant T., Faivovich J., Bain R.H., Haas A., Haddad C.F.B., de Sá R.O., Channing A., Wilkinson M., Donnellan S.C., Raxworthy C.J., Campbell J.A., Blotto B., Moler P., Drewes R.C., Nussbaum R.A., Lynch J.D., Green D.M., Wheeler W.C. 2006. The amphibian tree of life. *Bull. Am. Mus. Nat. Hist.* 297:1–370.
- Gao K.Q., Shubin N.H. 2001. Late Jurassic salamanders from northern China. *Nature* 410:574–577.
- Gao K.Q., Shubin N.H. 2003. Earliest known crown-group salamanders. *Nature* 422:424–428.
- Gardner J.D. 2003. The fossil salamander *Proamphiuma cretacea* Estes (Caudata: Amphiumidae) and relationships within the Amphiumidae. *J. Vertebr. Paleontol.* 23:769–782.
- Guindon S., Dufayard J.-F., Lefort V., Anisimova M., Hordijk W., Gascuel O. 2010. New algorithms and methods to estimate maximum likelihood phylogenies: assessing the performance of PhyML 3.0. *Syst. Biol.* 59:307–321.
- Jones R.W. 2011. *Applications of paleontology: techniques and case studies*. Cambridge: Cambridge University Press.
- Kozak K.H., Larson A., Bonett R.M., Harmon L.J. 2005. Phylogenetic analysis of ecomorphological divergence, community structure, and diversification rates in dusky salamanders (Plethodontidae: *Desmognathus*). *Evolution* 59:2000–2016.
- Kozak K.H., Mendyk R.W., Wiens J.J. 2009. Can parallel diversification occur in sympatry? Repeated patterns of body-size evolution in coexisting clades of North American salamanders. *Evolution* 63:1769–1784.
- Lanfear R., Calcott B., Ho S.Y., Guindon S. 2012. Partitionfinder: combined selection of partitioning schemes and substitution models for phylogenetic analyses. *Mol. Biol. Evol.* 29:1695–1701.
- Lanza B., Caputo V., Nascetti G., Bullini L. 1995. Morphologic and genetic studies of the European plethodontid salamanders: taxonomic inferences (genus *Hydromantes*). *Monografie XVI, Museo Regionale di Scienze Naturali, Torino*.
- Lanza B., Pastorelli C., Lagni P., Cimmaruta R. 2005. A review of systematics, taxonomy, genetics, biogeography and natural history of the genus *Speleomantes* Dubois, 1984 (Amphibia Caudata Plethodontidae). *Atti Mus. Civ. Stor. Nat. Trieste Suppl.* 52: 5–135.
- Lanza B., Vanni S. 1981. On the biogeography of plethodontid salamanders (Amphibia Caudata) with a description of a new genus. *Monit. Zool. Ital. (N.S.)* 15:117–121.

- Liu L., Yu L., Edwards S.V. 2010. A maximum pseudo-likelihood approach for estimating species trees under the coalescent model. *BMC Evol. Biol.* 10:302.
- Löytynoja A., Goldman N. 2008. A model of evolution and structure for multiple sequence alignment. *Philos. Trans. R. Soc. B* 363:3913–3919.
- Macey J.R. 2005. Plethodontid salamander mitochondrial genomics: a parsimony evaluation of character conflict and implications for historical biogeography. *Cladistics* 21:194–202.
- Min M.S., Yang S.Y., Bonett R.M., Vieites D.R., Brandon R.A., Wake D.B. 2005. Discovery of the first Asian plethodontid salamander. *Nature* 435:87–90.
- Mueller R.L., Macey J.R., Jaekel M., Wake D.B., Boore J.L. 2004. Morphological homoplasy, life history evolution, and historical biogeography of plethodontid salamanders inferred from complete mitochondrial genomes. *Proc. Natl. Acad. Sci. USA* 101:13820–13825.
- Mueller R.L. 2006. Evolutionary rates, divergence dates, and the performance of mitochondrial genes in Bayesian phylogenetic analysis. *Syst. Biol.* 55:289–300.
- Mulcahy D.G., Noonan B.P., Moss T., Townsend T.M., Reeder T.W., Sites Jr J.W., Wiens J.J. 2012. Estimating divergence dates and evaluating dating methods using phylogenomic and mitochondrial data in squamate reptiles. *Mol. Phylogenet. Evol.* 65:974–991.
- Near T.J., Eytan R.I., Dornburg A., Kuhn K.L., Moore J.A., Davis M.P., Wainwright P.C., Friedman M., Smith W.L. 2012. Resolution of ray-finned fish phylogeny and timing of diversification. *Proc. Natl. Acad. Sci. USA* 109:13698–13703.
- Pyron R.A. 2010. A likelihood method for assessing molecular divergence time estimates and the placement of fossil calibrations. *Syst. Biol.* 59:185–194.
- Pyron R.A. 2011. Divergence time estimation using fossils as terminal taxa and the origins of Lissamphibia. *Syst. Biol.* 60:466–481.
- Pyron R.A. 2014. Biogeographic analysis reveals ancient continental vicariance and recent oceanic dispersal in amphibians. *Syst. Biol.* 63:779–797.
- Pyron R.A., Wiens J.J. 2011. A large-scale phylogeny of Amphibia including over 2800 species, and a revised classification of extant frogs, salamanders, and caecilians. *Mol. Phylogenet. Evol.* 61:543–583.
- Rage J.C., Roček Z. 1989. Redescription of *Triadobatrachus massinoti* (Piveteau, 1936) an anuran amphibian from the early Triassic. *Palaeont. Abt. A* 206:1–16.
- Rambaut A., Drummond A. 2007. Tracer. Version 1.4. Available from: URL <http://beast.bio.ed.ac.uk/Tracer>.
- Ree R.H., Smith S.A. 2008. Maximum likelihood inference of geographic range evolution by dispersal, local extinction, and cladogenesis. *Syst. Biol.* 57:4–14.
- Roelants K., Gower D.J., Wilkinson M., Loader S.P., Biju S.D., Guillaume K., Moriau L., Bossuyt F. 2007. Global patterns of diversification in the history of modern amphibians. *Proc. Natl. Acad. Sci. USA* 104:887–892.
- Ronquist F., Teslenko M., van der Mark P., Ayres D., Darling A., Hohns S., Larget B., Liu L., Suchard M.A., Huelsenbeck J.P. 2012. MrBayes 3.2: efficient Bayesian phylogenetic inference and model choice across a large model space. *Syst. Biol.* 61:539–542.
- Ruben J.A., Boucot A.J. 1989. The origin of the lungless salamanders (Amphibia: Plethodontidae). *Amer. Nat.* 134:161–169.
- Scotese C.R. 2001. PALEOMAP Project, Arlington, Texas, Version 02b. Available from: URL <http://www.scotese.com>.
- Shen X.X., Liang D., Feng Y.J., Chen M.Y., Zhang P. 2013. A versatile and highly efficient toolkit including 102 nuclear markers for vertebrate phylogenomics, tested by resolving the higher level relationships of the Caudata. *Mol. Biol. Evol.* 30:2235–2248.
- Shimodaira H., Hasegawa M. 2001. CONSEL: for assessing the confidence of phylogenetic tree selection. *Bioinformatics* 17: 1246–1247.
- Springer M.S., Murphy W.J., Eizirik E., O'Brien S.J. 2003. Placental mammal diversification and the Cretaceous–Tertiary boundary. *Proc. Natl. Acad. Sci. USA* 100:1056–1061.
- Stamatakis A. 2006. RAxML-VI-HPC: maximum likelihood-based phylogenetic analyses with thousands of taxa and mixed models. *Bioinformatics* 22:2688–2690.
- Swofford D.L. 2002. PAUP* Phylogenetic analysis using parsimony (*and other methods). Version 4.0b10 ed. Sunderland, MA: Sinauer Associates.
- Tamura K., Peterson D., Peterson N., Stecher G., Nei M., Kumar S. 2011. MEGA5: molecular evolutionary genetics analysis using maximum likelihood, evolutionary distance, and maximum parsimony methods. *Mol. Biol. Evol.* 28:2731–2739.
- Tan G., Muffato M., Ledergerber C., Herrero J., Goldman N., Gil M., Dessimoz C. 2015. Current methods for automated filtering of multiple sequence alignments frequently worsen single-gene phylogenetic inference. *Syst. Biol.* 0(0):1–14.
- Tiffney B.H. 1985. The Eocene North Atlantic land bridge: its importance in Tertiary and modern phytogeography of the Northern Hemisphere. *J. Arnold Arb.* 66:243–273.
- Tiffney B.H., Manchester S.R. 2001. The use of geological and paleontological evidence in evaluating plant phylogeographic hypotheses in the Northern Hemisphere Tertiary. *Int. J. Plant. Sci.* 162:S3–S17.
- Thorne J.L., Kishino H. 2002. Divergence time and evolutionary rate estimation with multilocus data. *Syst. Biol.* 51:689–702.
- Tihen J.A., Wake D.B. 1981. Vertebrae of plethodontid salamanders from the lower Miocene of Montana. *J. Herp.* 15:35–40.
- Venczel M., Sanchíz B. 2005. A fossil plethodontid salamander from the Middle Miocene of Slovakia (Caudata, Plethodontidae). *Amphibia-Reptilia* 26:408–411.
- Vieites D.R., Min M.S., Wake D.B. 2007. Rapid diversification and dispersal during periods of global warming by plethodontid salamanders. *Proc. Natl. Acad. Sci. USA* 104:19903–19907.
- Vieites D.R., Nieto-Román S., Wake M.H., Wake D.B. 2011. A multigenic perspective on phylogenetic relationships in the largest family of salamander, the Plethodontidae. *Mol. Phylogenet. Evol.* 59: 623–635.
- Wake D.B., Maxson L.R., Wurst G.Z. 1978. Genetic differentiation, albumin evolution, and their biogeographic implications in plethodontid salamanders of California and southern Europe. *Evolution* 32:529–539.
- Wake D.B. 1966. Comparative osteology and evolution of the lungless salamanders, Family Plethodontidae. *Mem. South Calif. Acad. Sci.* 4:1–111.
- Wake D.B. 1991. Homoplasy: the result of natural selection, or evidence of design limitations? *Amer. Nat.* 138:543–567.
- Wake D.B. 2009. What salamanders have taught us about evolution. *Ann. Rev. Ecol. Evol. Syst.* 40:333–352.
- Wake D.B. 2012. Taxonomy of salamanders of the Family Plethodontidae (Amphibia: Caudata). *Zootaxa* 3484:75–82.
- Wake D.B. 2013. The enigmatic history of the European, Asian and American plethodontid salamanders. *Amphibia-Reptilia* 34: 323–336.
- Wiens J.J., Engstrom T.N., Chippindale P.T. 2006. Rapid diversification, incomplete isolation, and the “speciation clock” in North American salamanders (genus *Plethodon*): testing the hybrid swarm hypothesis of rapid radiation. *Evolution* 60:2585–2603.
- Wiens J.J. 2007. Global patterns of diversification and species richness in amphibians. *Amer. Nat.* 170:S86–S106.
- Wilder I.W., Dunn E.R. 1920. The correlation of lunglessness in salamanders with a mountain brook habitat. *Copeia* 84: 63–68.
- Yang Z. 2007. PAML 4: phylogenetic analysis by maximum likelihood. *Mol. Biol. Evol.* 24:1586–1591.
- Zachos J., Pagani M., Sloan L., Thomas E., Billups K. 2001. Trends, rhythms, and aberrations in global climate 65 Ma to present. *Science* 292:686–693.
- Zhang P., Wake D.B. 2009. Higher-level salamander relationships and divergence dates inferred from complete mitochondrial genomes. *Mol. Phylogenet. Evol.* 53:492–508.
- Zhang P., Zhou H., Chen Y.Q., Liu Y.F., Qu L.H. 2005. Mitogenomic perspectives on the origin and phylogeny of living amphibians. *Syst. Biol.* 54:391–400.
- Zheng Y.C., Peng R., Masaki Kuro-o M., Zeng X.M. 2011. Exploring patterns and extent of bias in estimating divergence time from mitochondrial DNA sequence data in a particular lineage: a case study of salamanders (order Caudata). *Mol. Biol. Evol.* 28: 2521–2535.
- Zhu T., dos Reis M., Yang Z. 2015. Characterization of the uncertainty of divergence time estimation under relaxed molecular clock models using multiple loci. *Syst. Biol.* 64:267–280.